Journal of Cleaner Production 509 (2025) 145536

Contents lists available at ScienceDirect

Journal of Cleaner Production

journal homepage: www.elsevier.com/locate/jclepro

Spatially explicit freshwater eutrophication potential (EP) from water resource recovery facility (WRRF) discharge and mitigation opportunities in the U.S.

Karla G. Morrissey [a,*], Andrew D. Henderson [b,c], John Zimmerman [a], Greg Thoma [a,d]

[a] Department of Chemical Engineering, 1 University of Arkansas, Fayetteville, AR, 72701, USA
[b] Eastern Research Group, ERG, Concord, MA, 01742, USA
[c] École de Technologie Supérieure, Montréal, QC, H3C 1K3, Canada
[d] AgNext, Colorado State University, Fort Collins, CO, 80523, USA

ARTICLE INFO

Handling Editor: Maria Teresa Moreira

Keywords:
Nutrient recovery
Water resource recovery facilities
Wastewater treatment
Spatially explicit freshwater eutrophication potential
Site-specific characterization factors

ABSTRACT

While technologies are in development to recover key, non-renewable nutrients and reduce eutrophication potential from wastewater treatment, there currently does not exist information that can inform an effective strategy to maximize the impacts of these efforts while maintaining efficient use of limited resources. This work provides 1) an estimate of spatially explicit emitted EP (EP_E) from WRRFs in the contiguous U.S. at 0.5-degree resolution using total P emissions from WRRFs and site-specific cumulative fate factors from a global model, 2) conceptualization and estimate of total spatially explicit received EP (EP_R) locally and upstream for each grid cell, 3) estimate of percent EP_R from local vs. upstream sources for each grid cell, 4) hotspot analysis and impact assessment of EP mitigation via nutrient recovery in a case study. Mapping grid cells with site-specific EP_E show hotspots near the Great Lakes area, where P emissions from WRRFs and/or cumulative fate factors are high and yield the highest EP_E. Estimates for received EP show nearly half of all non-arid cells in the U.S. with P loading have the majority of spatially explicit EP_R stemming from local WRRF discharge rather than upstream WRRFs. Grid cells with a majority of EP_R coming from upstream sources, as opposed to local sources, tended to occur in areas near or encompassing rivers. These results also showed that when focusing only on cells that encompassed 303(d) listed impaired waters, most cells receive more than half of their EP_R from local sources. Case study results show that of the 19 grid cells that contribute to the mouth of Wabash River, three cells contribute 52 % of the total EP_R. When modeling a 25 % reduction in P emissions of contributing cells, it is found that similar EP_R reductions could be achieved at the mouth of the river from two of the largest contributing cells; however, this 25 % reduction in one cell equated to less than half overall P reduction (lb P emitted) compared to the other contributing cell.

1. Background

Phosphorus is a vital, non-renewable nutrient required to sustain life, and global reserves are being depleted (Cordell et al., 2009). More than 90 % of mined phosphorus is used to make fertilizer to grow food, in a linear system: the recovery and reuse of phosphorus is not yet implemented at scale. Therefore, there are predictions that phosphorus shortages will put the global food supply at risk in the coming century (al Rawashdeh and Maxwell, 2011). Furthermore, discharge of phosphorus into freshwater systems is negatively impacting lakes and rivers, as well as the U.S. economy (Dodds et al., 2009; US EPA, 2015a). When phosphorus is discharged in aquatic systems, it promotes algae growth that can cause harmful algal blooms and "dead zones; " this process is referred to as eutrophication (Bhat and Qayoom, 2021). Nationwide, 45 % of lakes have elevated phosphorus levels (24 % of lakes have hyper-eutrophic conditions), while 58 % of rivers have elevated phosphorus levels (US EPA, 2022a, 2020). Eutrophication damages in the US were estimated at $2.2 billion USD in 2009 ($3.15 billion 2003 USD) annually, likely underestimating total freshwater impacts (Dodds et al., 2009).

Phosphorus poses problems at both extraction and at use: resource depletion and environmental impacts. The resource recovery problem

* Corresponding author.
E-mail address: karlamorrissey@gmail.com (K.G. Morrissey).

https://doi.org/10.1016/j.jclepro.2025.145536
Received 31 October 2024; Received in revised form 3 April 2025; Accepted 15 April 2025
Available online 25 April 2025

has been addressed by prioritizing identification of key sources of phosphorus in its anthropogenic cycle for nutrient recovery. A review of phosphorus flow analyses published between 2005 and 2012 identified key outflows of P in cities and regions/nations as wastewater discharge, landfills, and soil losses through erosion, runoff, and leaching (Chowdhury et al., 2014). Wastewater in particular has been identified as a potential opportunity for recovery of phosphorus as humans excrete nearly all of the phosphorus they consume (Jönsson et al., 2004). In fact, research has suggested enormous potential: if 100 % of the phosphorus available in human waste and animal manure in the U.S. were recovered, 130 % of U.S. fertilizer demand would be met (Jarvie et al., 2015). The environmental impact of phosphorus has been addressed by prioritizing mitigation of eutrophication potential (EP) in aquatic ecosystems. Although N, P, and other constituents can contribute to eutrophication, P is typically the limiting nutrient in temperate freshwater systems (Chorus and Spijkerman, 2021; Wurtsbaugh et al., 2019), though N certainly plays a role (Dodds and Smith, 2016). Location is vital for both resource recovery and ecosystem damage perspectives. EP is heavily influenced by locations of point-source loading, non-point source loading, local and upstream hydrological characteristics, and existing water quality conditions. There are also temporal variations in P contributions to eutrophication. Temperature fluctuation, lake stratification, and changing flow regimes contribute to such variations (Henderson, 2015). Large-scale quantification of these variations is still limited. For example, an evaluation of phosphorus fate in Brazil suggested that seasonal, rather than monthly, variations are important in modeling (de Andrade et al., 2021).

Modeling tools such as the SPAtially Referenced Regression On Watershed attributes (SPARROW) model have focused on assessing watershed quality through quantification of nutrient loading to U.S. lakes and rivers (Preston et al., 2011b). The SPARROW model has been used to simulate phosphorus fate in several regions in the U.S., and in some studies, identified municipal and industrial wastewaters as key sources of nutrients in the Northeast and upper Midwest (Moore et al., 2011; Robertson and Saad, 2019). While there has been notable work over large scales using regression models, such as SPARROW (e.g., Preston et al., 2011a), mechanistic phosphorus models are typically applied over limited spatial scales. There are other examples of mechanistic models over large regions, e.g., a 1×1 km eutrophication model for nitrogen in the Guangzhou, China region, though this model used population density as a proxy for wastewater emissions (Dong et al., 2023).

These perspectives (resource recovery and ecosystem damage) coincide at water resource recovery facilities (WRRFs), as WRRF discharge is one of the largest sources of P into some freshwater systems as well as one of the primary sources from which we can recover phosphorus (Rahman et al., 2019). In recent decades, nutrient recovery technologies have been developed to effectively recover P-containing products from urine/liquid phase streams, sludge, or sludge ash, in both centralized and decentralized wastewater treatment (WWT) (Corominas et al., 2013; Lam et al., 2020; Sena and Hicks, 2018). Life cycle assessment (LCA) and life cycle impact assessment (LCIA) has been used to quantify environmental impacts, including EP, from implementing both emerging and mature nutrient recovery technologies, primarily at the facility level (Amann et al., 2018; Egle et al., 2016; Johansson et al., 2008; Linderholm et al., 2012; Morrissey et al., 2022; Remy and Jossa, 2015; Rodriguez-Garcia et al., 2014; Sena et al., 2021). One study calculated reductions of bioavailable N and P in WRRF discharge for 10 different WWT configurations to identify the treatment schemes that remove the most bioavailable N and P, but did not estimate actual EP impacts (Preisner et al., 2021). Another study estimated changes to the N and P cycles from varying levels of WWT at the global scale (Wang et al., 2019). Although local evaluations of EP from WRRF discharge and national estimates of EP from WRRF discharge have been performed, the former are typically restricted in their spatial coverage, and the latter have been restricted in their spatial resolution. As mentioned previously, eutrophication impacts are site-specific – an emission of an equal mass of phosphorus in one location may have significantly different EP effects compared to the same mass emitted at another location. Additionally, no known systematic, large-scale studies have disaggregated these EP estimates at a specific location to provide detailed information regarding the source of the phosphorus loading—whether it is emitted within the local geographic boundary or from an upstream region. Finally, systematic, large-scale potential reductions to spatially explicit EP in water bodies from WRRF discharge, especially nutrient impaired waters, have not been modeled. With a variety of effective P-recovery technologies available for WWT, including advanced treatment configurations, the focus must now turn to creating an effective P-recovery and EP reduction strategy in which the greatest reductions to site-specific EP can be realized while conserving this essential element, as well as other limited resources. An effective strategy will include 1) a current assessment of EP from WRRF discharge, 2) determination of EP "hotspots" and origins of P loadings (local vs. upstream contributions) with special attention given to nutrient impaired waters, and 3) modeling of potential reductions in EP loading from implementation of nutrient recovery technology. The purpose of this study is to conduct these assessments focusing on EP from WRRF discharge in the United States with the aim of providing useful data that can help shape an effective strategy for conserving phosphorus and mitigating EP.

2. Methods

2.1. Goal and scope

The goals of this assessment were to 1) determine current spatially explicit EP impacts in the U.S. from WRRF discharge, 2) determine hotspots in EP and differentiate local vs. upstream P contributions to EP with an additional assessment of the EPA 303(d) listed nutrient impaired waters, and 3) model potential changes in spatially explicit EP from hypothetical P recovery in treatment plants to an impaired water in an example case study. The scope of this study includes freshwater EP calculated solely from WRRF discharge in the U.S., using public data for P emissions from WRRF, but the method is applicable more broadly, provided data are available. With a focus on evaluating benefits of hypothetical P recovery at the national level, we perform the analysis based on annual emissions of P. This evaluation of P recovery uses impact assessment models from LCIA, but as it takes spatially distributed WRRF P emissions as the starting point, it does not constitute a classic LCA of e.g., WWT.

It is important to note that non-point sources including fertilizer runoff as well as P flows from land-applied sludge can significantly affect EP. In some cases, non-point sources can be the largest contributors to EP. However, state-level information for biosolids disposal in the U.S is site-generic, providing no geospatial information for land application of biosolids applied. Thus, P flows from land application of sludge were not included in the quantification of spatially explicit EP in this study. Additionally, nitrogen flows were not included in this analysis, nor were marine eutrophication impacts assessed. While these flows were not included, this work is relevant because we 1) establish the methodology to conduct a novel spatially-explicit analysis of freshwater eutrophication from WRRFs that can be further expanded to model additional P flows, provided that data is available, and 2) enable identification of key WRRFs that largely contribute to local and downstream eutrophication and thus could serve as ideal candidates for advanced nutrient recovery technology.

2.2. Definition of terms and calculations

In this section, we define several terms used in this study to provide clarification of concepts and calculations. Firstly, a distinction is made between "emissions" and "loading." In this study, the term "emissions" refers to P flows directly from WRRFs within the geographic boundary of a local compartment; that is, emissions refer to local discharges of phosphorus. "Loading" refers to all releases of phosphorus entering a defined geographic boundary, which includes both local discharge (emissions) as well as phosphorus flows from upstream sources entering the geographic compartment of interest (advective loadings). "Upstream sources" refer to P entering a receiving compartment that is exogenous of the geographic boundary of the receiving compartment.

Additionally, it is important to define spatially explicit EP and terms used to calculate EP from an LCIA perspective. In LCIA, EP is a midpoint impact relating a steady-state mass flow (P loading, i.e., emission) to a change in steady-state mass in receiving compartment (Henderson et al., 2021; Jolliet et al., 2004). Spatially explicit EP is calculated by multiplying a P flow by a spatially explicit fate factor (FF). A spatially explicit FF for phosphorus estimates the persistence of P emissions, or residence time, in a compartment based on site-specific removal processes including losses via water use, retention in sediment, and removal downstream through advection (Helmes et al., 2012). FFs have units of time (mass in compartment/mass released. time^{-1}), and the unit chosen for this study is years. The effect factor is not included in the definition of spatially explicit EP at the midpoint level. An effect factor (EF) in EP relates the emission of P to its potential ecological damage to a compartment, and is more commonly applied to endpoint characterization (Bulle et al., 2019; Helmes et al., 2012). With the addition of spatially explicit effect factors for freshwater eutrophication, future studies can focus on calculating end-point impacts from WRRF discharge. However, this study focuses solely on spatially explicit EP midpoint impacts, with P flows multiplied by spatially explicit FFs (Helmes et al., 2012). Global spatially explicit FFs for P flows used in this study are provided by Helmes et al. for grid cells at 0.5° spatial resolution (~50 km × 50 km cells at mid-latitudes). Despite recent improvements in eutrophication modeling at local and regional scales (Zhuang et al., 2024), there are no phosphorus fate models with higher spatial or temporal resolution available for areas as large as the U.S.

FFs can be further classified as either individual or cumulative. An individual FF describes the persistence of P in a single receiving cell. A cumulative FF is a combination of multiple, hydrologically connected cells, and thus depends on transfer fractions between those cells. A transfer fraction is dimensionless and defined as the percentage of a P flow that is transmitted from an upstream cell to a downstream cell via advection. An emission originating from cell *i* has a transfer fraction of 1.0 to cell *i* (100 % of the emission within the cell is transferred to itself). We make a distinction between individual transfer fractions and cumulative transfer fractions. If a cell has a downstream receiving cell, the individual, or cell-to-cell, transfer fraction defines the fraction of P that is transmitted from emitting cell *i* to receiving cell *j* (adjacent). A cumulative transfer fraction calculates the fraction of P that is received in a cell not adjacent to the emitting cell by taking the product of the individual transfer fractions of all cells connecting the emitting cell to the receiving cell. Then, a cumulative (downstream) FF for a given cell (FF_i) is defined as the sum of the product of cumulative downstream transfer fractions and respective individual FFs, as shown in Equation (2) (Helmes et al., 2012):

$$FF_i[years] = \sum_{j=i}^{n} f_{i,j}[dimensionless] * \tau_j[years] = \sum_{j=i}^{n} FF_{i,j}[years] \quad (1)$$

where cell *i* is the index of the emitting, or upstream, cell, cell *j* is the index of receiving, or downstream, cells, $f_{i,j}$ is the cumulative transfer fraction of P from cell *i* to cell *j*, τ_j is the residence time of P in cell *j*, and $FF_{i,j}$ is the FF from emission in upstream cell *i* to receiving cell *j* (Helmes et al., 2012). The sum of j is over the emitting cell (*i*) and all downstream cells (i.e., up to and including the last cell, *n*).

Lastly, a distinction is made between EP from an *emitting* perspective, and EP from a *receiving* perspective. EP from an emitting perspective, hereby referenced as EP_E, represents spatially explicit impacts from P *emissions* in an emitting cell multiplied by spatially explicit cumulative FFs (discussed further in Section 2.3), and as shown in Equation (1). This cumulative "emission" perspective is frequently, if not exclusively, used in characterization of eutrophication, as it combines the local and downstream EP of an emission (the EP in this framework is assigned to the cell where the emission occurs). EP from a receiving perspective, hereby referenced as EP_R, calculates total EP in a receiving compartment, including EP from local P emissions *and* upstream P sources (discussed further in Section 2.4). The EP_R perspective is novel in the application of LCA-based FFs. We note that EP_E and EP_R are two distinct perspectives that are not meant to be added or otherwise quantitatively related; rather either perspective can be used depending on the focus of an analysis.

2.3. Spatially explicit EP_E in the U.S. From WRRF discharge

For the first objective, U.S. WRRF data including latitude, longitude, and P emissions were obtained from the EPA Nutrient Modeling (Hypoxia Task Force Search) Tool (US EPA, 2022b). The search criteria were set to include P loadings from 'Publicly Owned Treatment Works (POTWs) Only' with the exception of including industrial facilities that also treat domestic sewage. No other limiting parameters were defined. The tool exported 17,020 WRRFs in the U.S. These plants were mapped using the latitude and longitude reported for each plant. Next, these points were matched to cells in the 0.5 × 0.5° network of the FF model (Helmes et al., 2012). The number of treatment plants per cell (count), their cumulative local phosphorus emissions, and minimum and maximum emissions were calculated using the 'Aggregate Points' tool. These cells were joined with the global FFs (Helmes et al., 2012) to create a new table with 2255 cells, each with individual and cumulative FFs, transfer fractions and P emissions data if available. Of these cells, 451 had null values for their cumulative FF; these factors show that these cells are arid and evapotranspiration potential exceeds precipitation. Additionally, 71 cells had no local phosphorus emissions. A new "EP" field was created in the joined attribute table to represent spatially explicit EP_E. The calculation for EP_E in cell i is shown in Equation (1):

$$EP_{E,i}\left[lbs\ P_{eq}\right] = P_i\left[\frac{lbs\ P}{year}\right] * FF_i[years] \quad (2)$$

where $P_i = \sum_{k=1}^{N} P_k$, or the cumulative P emissions from sources, *k*, located within emitting cell *i*. FF_i is the cumulative FF (i.e., accounting for FF in cell *i* and downstream) for P emitted in cell *i*.

A classification map was generated in ArcGIS Pro to show the spatially explicit EP_E in the U.S. calculated from Equation (1) specifically from WRRF discharge. The population in each grid cell was also determined to aid interpretation. A raster file for global population was obtained from the Global Human Settlement Layer (GHSL), clipped to U. S. boundaries, and converted to a point feature layer (Florczyk et al., 2019; Freire et al., 2019). Similar to the treatment plant point feature layer, this layer was aggregated to the grid cells from Helmes et al. and the total population was calculated for each cell. A table ranking the top 10 cells by total EP is provided. A table with all 1733 cells ranked by EP_E is included in the supplementary material (Table S1).

2.4. Determination of local and upstream contributions to EP_R

For the second objective, a "receiving" perspective is particularly useful for our current application, as it disaggregates the total EP_R in each cell into local and upstream contributions. Mathematically, a receiving FF can be calculated as in Equation (2), above, but this calculation is of limited use, as it implicitly uses a unit emission in all upstream cells. However, total EP_R in a receiving cell *j* can be calculated by including exogenous P loading arriving from upstream cells, *i*, as shown in Equation (3):

$$EP_{R,j}\left[lbs\ P_{eq}\right] = \sum_{i=j}^{\substack{cell\ j\ and\ all\ cells\\ upstream\ of\ j}} FF_{i,j} * P_i \tag{3}$$

where i are all cells upstream of a receiving cell j, $FF_{i,j}$ is as in Equation (1), the FF from emission in upstream cell i to receiving cell j. Thus, $FF_{i,j} * P_i$ is the loading-adjusted phosphorus emission in cell i reaching cell j. In contrast to the emission (downstream) perspective, where each cell discharges to one cell only, there may be branches upstream of a receiving cell. The fraction of local and upstream emissions may be calculated relative to EP_R. A map was generated to show local vs. total EP_R for all 1733 cells in the U.S. that have both P loading and FF data.

2.5. EPA 303(d) listed nutrient impaired waters

This study also includes a closer analysis of nutrient impaired waters in the U.S. to assess current EP_R and their sources. A list of EPA 303(d) listed impaired waters was obtained from the NHDPlus Indexed Dataset with Program Attributes (US EPA, 2015b). A total of 49,876 listings were obtained with information including Total Maximum Daily Load (TMDL) ID, cycle year, listed water ID, 'Parent_Pollutant' group, and TMDL 'Pollutant_Name.' This list was reduced to include listings with 1) "Point source" or combined "Point source/nonpoint Source" listings, 2) a TMDL Parent_Pollutant of "Nutrients," and 3) a TMDL Pollutant_Name of "Phosphorus." In order to map this reduced list of 303(d) listed waters, hydrologic unit code (HUC) data was obtained. To our knowledge, there is no current database that allows for automatic matching between 303(d) listed impaired waters with HUC data. To match listings to HUC-12 data, we used python-based scripts (Zimmerman, 2021). A map of 303(d) listed impaired waters meeting our criteria (444 listings) were mapped as points, lines, or polygons based on their reported geographic attributes. The intersection of 303(d) listings with the gridded FF cells provided a list of all grid cells containing impaired waters. Local vs. upstream contributions to EP_R were mapped separately to provide additional insight into the potential interventions that may be relevant for specific impaired locations.

2.6. Case study: nutrient recovery in WRRFs upstream of the Wabash River in Indiana

With knowledge of the relative contribution of total EP from local vs. upstream sources, we can make more informed decisions in determining the most relevant WRRFs for phosphorus-reducing intervention such as implementation of nutrient recovery technologies. Here we describe a case study to demonstrate how these data can be used to mitigate EP most effectively for a 303 (d) nutrient impaired river. A portion of the Wabash River in Indiana was chosen for the case study in this analysis as it contains cells with a wide range of local to total EP contributions (described further in Section 3.4). Choosing a point just downstream of Indianapolis, IN as the downstream boundary of the watershed (the outlet of the study area), a list of all upstream contributing cells was determined using the Helmes et al. flow data (Helmes et al., 2012). Total spatially explicit EP_R was calculated for the cell encompassing the mouth of the river using Equation (3) with FFs and transfer fractions for all contributing cells. Once total EP_R was calculated, disaggregation of EP_R by contributing cell was estimated. Percent contributions to the total EP_R at the outlet of the Wabash River case study area from each upstream cell were calculated and compared to determine key contributing cells. Once these cells were identified, theoretical nutrient reductions were modeled to determine potential EP_R changes to the receiving cell based on assumed nutrient reduction in each contributing cell.

3. Results and discussion

3.1. Spatially explicit EP_E from WRRF discharge

Fig. 1 presents a map with graduated colors reflecting spatially explicit combination of phosphorus fate and loading, i.e. the EP (lb P-eq), from WRRF discharge in the U.S.

High EP_E from plant discharge is shown by orange and red grid cells; these cells exhibit either 1) high phosphorus loading from discharge, 2) large cumulative FFs, or both. While high phosphorus loading may be influenced by a variety of factors (population density, high industrial activity/loading, etc.), a high cumulative FF indicates that P loading from a particular grid cell will have a higher overall residence time in receiving and downstream freshwater streams compared to grid cells with lower cumulative FFs. Some of the highest EP cells are in the Great lakes area (Chicago, Milwaukee, Detroit, Cleveland and Buffalo), but other metro areas (Jacksonville, Kansas City, Jefferson City, Tulsa, Memphis, Houston, and Dallas) are among the top cities. To the west, there are fewer grid cells shown as a) population density is lower, and there are regions with 0 WRRF loading, and b) this region of the U.S. is more arid (grid cells have a null FF) than the eastern U.S. Regarding the latter, a null cumulative FF signifies that evapotranspiration rates exceed precipitation; therefore, in the model, no phosphorus is transferred to a downstream cell (we recognize that seasonal flows may indeed transport P in these areas). Hotspots in the west include Salt Lake City, San Diego, and Seattle.

These results provide an overview of current site-specific EP_E to U.S. water bodies specifically from WRRF discharge and highlight key areas where EP_E are driven by either P flows and/or hydrologic conditions allowing for easy transfer of P to downstream cells. Table 1 shows the top 10 grid cells with the largest EP_E from wastewater plant discharge along with the grid cell population, total P loading to the cell, and the cell's cumulative FF.

The grid cell that includes the Chicago area (51015) has EP_E an order of magnitude higher than the grid cell with the second highest EP_E. High EP_E in this cell results from both high P emissions to this cell as well as a cumulative FF that is higher than almost all other FFs shown in Table 1. Interestingly, grid cell 50404 (outside of St. Louis) has almost 25 times the amount of phosphorus emissions from WRRF discharge compared to the Chicago-area grid cell; however, the cumulative FF for this cell is two orders of magnitude smaller, providing only one-fourth of the EP_E compared to cell 51015. Grid cells 51123 and 49019 have similar values for annual phosphorus emissions but vary in EP_E by 8,000,000 lb P. These results highlight how EP_E can change significantly when site-specific characterization factors are used instead of site generic factors. With the inclusion of site-specific FFs, EP_E can be estimated and used to prioritize locations of WRRFs for which advanced nutrient removal/recovery may be most environmentally beneficial. Fig. 2 shows each grid cell's EP_E as bubble size, plotted against phosphorus emissions (x-axis) and cumulative FF (y-axis).

A wide range of sizes for EP_E is shown in Fig. 2, with most data between P loading of 10,000 and 10 million lbs P per year. Cumulative FFs ranged between 0 and 10 years. Treatment plants with lower FFs typically showed smaller and similar values of EP_E despite the P loading spanning two orders of magnitude, ranging between 10,000–1,000,000 lb P loading/year. Some exceptions include the third largest EP_E bubble with nearly 100,000,000 lb P loading per year (grid cell 50404 between St. Louis and Jefferson City, MO). Conversely, WRRFs with lower P loading values (1000–10,000 lb P/yr) had smaller values of EP_E despite having cumulative FFs ranging between 1 and 10 years.

3.2. Spatially explicit EP_R from WRRF P loading in the U.S

A map showing the ratio between local to total EP_R in non-arid grid cells is shown in Fig. 3. This map only includes cells that are both non-arid and have a non-zero phosphorus loading (either all upstream, all

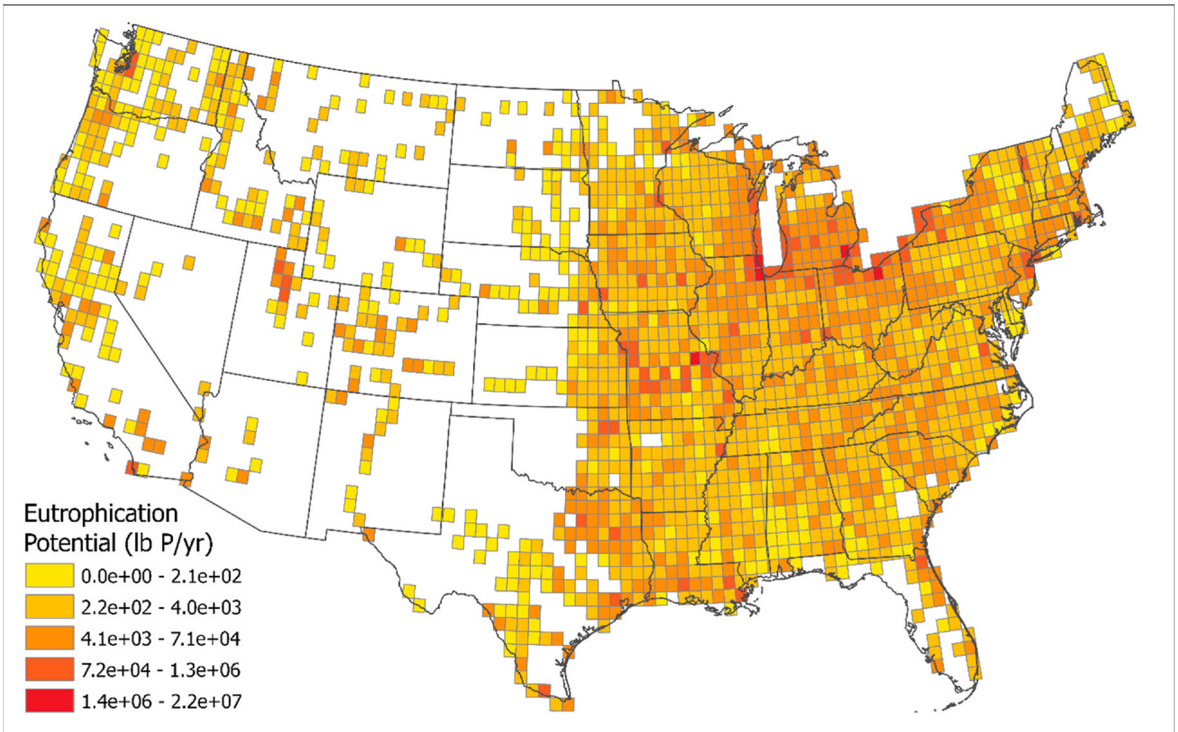

Fig. 1. Spatially explicit EP_E in the U.S. from WRRF discharge.

Table 1
Top 10 grid cells with EP_E from WRRF discharge.

Grid Cell (City, ST)	Population (millions)	Number of WRRFs	Cumulative P Loading (million lbs/yr)	Cumulative FF (yr)	EP (million lbs Peq)
51015 (Chicago, IL)	4.25	26	4.31	5.18	22.3
51123 (Evanston, IL-north of Chicago)	1.19	11	1.69	5.31	8.96
50404 (Between St. Louis and Jefferson City, MO)	0.0688	33	97.3	0.0613	5.97
50923 (Cleveland, OH)	1.34	42	0.971	1.81	1.76
51132 (Detroit, MI)	1.81	16	0.757	2.05	1.55
50,760 (Salt Lake City, UT)	1.00	8	1.03	1.18	1.21
48941 (Houston)	2.72	180	3.13	0.345	1.08
49019 (Jacksonville, FL)	0.996	23	1.59	0.629	0.998
50405 (St. Peters, MO-west of St. Louis)	0.586	55	16.1	0.0588	0.949
51122 (Crystal Lake, IL-northwest of Chicago)	1.13	38	7.37	1.80	0.941

local emissions, or a mix of the two).

A total of 1767 cells are both non-arid and have non-zero loading. The purple and dark colors show cells that have a larger ratio of upstream contributions to EP_R as opposed to EP_R arising from local emissions, with some of these cells (34, in black) receiving nearly all EP_R from upstream cells (local:total ratio <0.01). Cells encompassing river segments tend to have these darker colors instead of lighter orange or yellow colors, showing that for some bodies of water, EP_R is primarily driven from upstream P emissions, not local P emissions (that is, local WRRFs discharging to the river). Red, orange and yellow cells show a higher ratio of the total EP_R is coming from P emissions within the cell (local) versus upstream contributions; cells with EP_R stemming only from local P emissions and no upstream contributions are yellow and have a local:total ratio of 1.0. This map also shows that most non-arid cells (952) receive 87 % or more of their EP_R from local emissions rather than upstream loading. Of these cells, 832 have a local to total EP_R loading ratio of 1.0. Based on these estimates, we observe that nearly half of all non-arid cells in the U.S. with P loading have the majority of spatially explicit EP_R from local WRRF discharge rather than upstream WRRFs. For these cells, efforts to reduce EP_R loading from WRRF discharge can focus on local WRRF discharge contributions to total P loading. Key WRRFs that discharge a certain percent contribution (i.e. 10 % or higher, depending on the focus of investigation), can be targeted as ideal plants to implement advanced nutrient removal.

3.3. EPA 303(d) listed impaired waters

A total of 444,303(d) listed nutrient impaired waters were identified and mapped (see Fig. 4); these consist of a combination of point, line and area data points to represent water bodies from total maximum daily load (TMDL) data. Of these, 20 impaired waters were modeled as points (primarily creeks and ponds) and 285 waters were mapped as polygons (primarily lakes). Rivers and streams were modeled as a collection of line segments (2087 segments; multiple segments used to map one river or stream). When intersected with grid cells at 0.5° resolution, 155 cells were found to encompass these waters. Fig. 5 below shows a heat map representing local:total EP_R contributions to these cells with nutrient impaired waters. These waters are impaired due to a wide range of upstream and local P sources.

Of the 155 cells, 131 cells were paired with received EP and local:

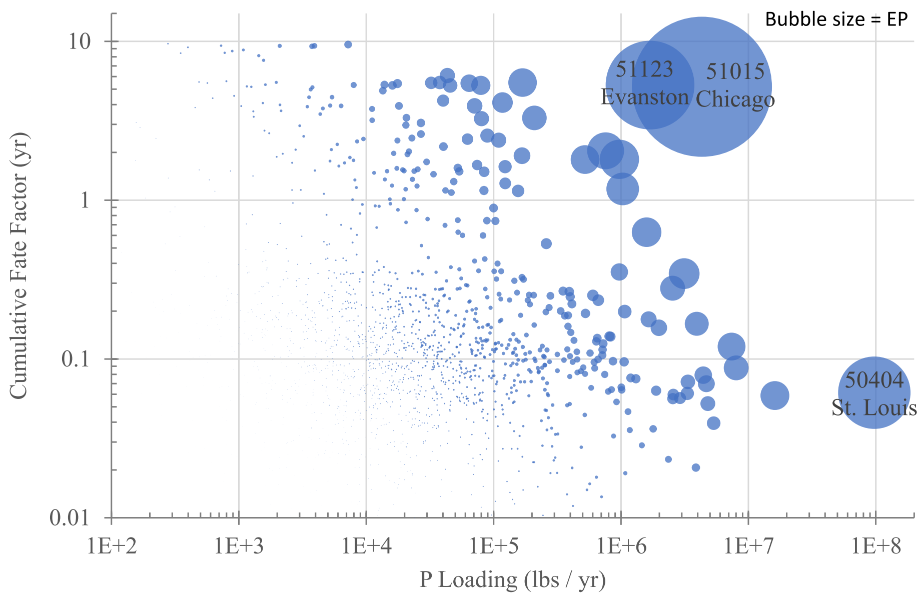

Fig. 2. Spatially explicit EP_E vs. P loading and cumulative FF; bubble size indicates EP, with the largest (Chicago) EP = 22.3M lbs P.

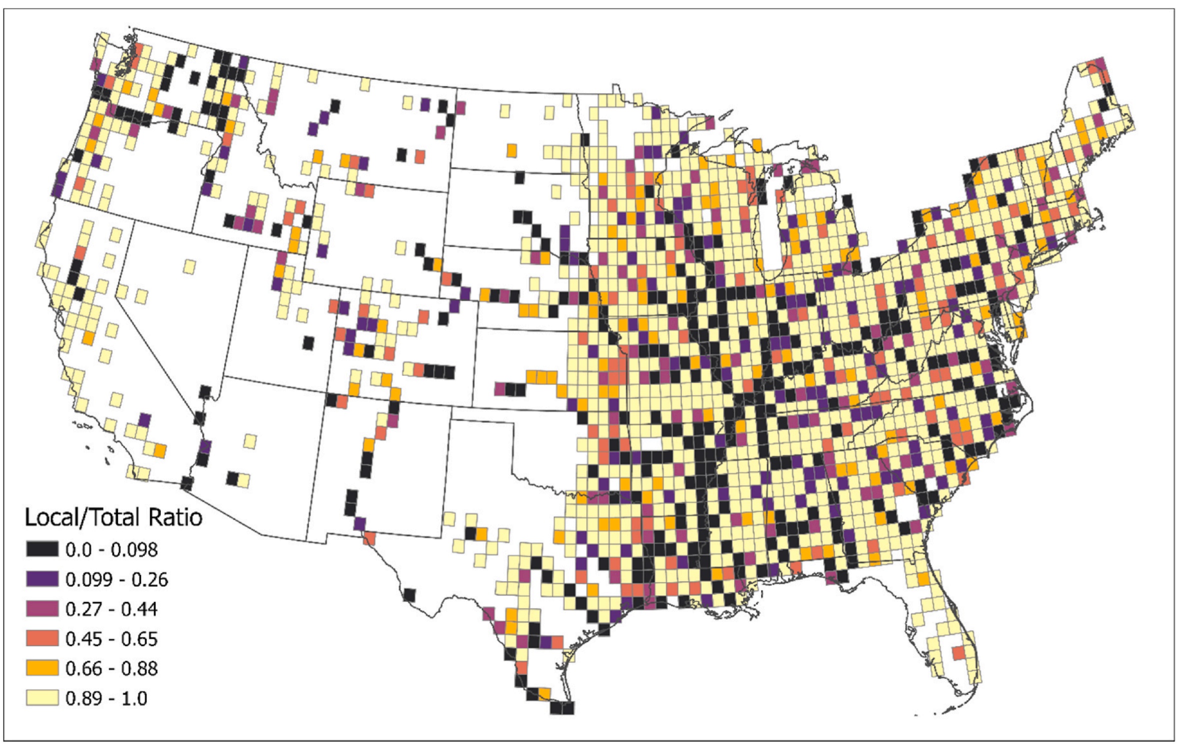

Fig. 3. Heat map of local vs. total EP_R for all cells in the U.S. (non-arid).

total EP_R ratios. Fourteen cells with nutrient impaired waters had null cumulative FFs. These cells reflect a disconnect between the capabilities of a global model and local conditions: arid cells are not necessarily devoid of water, though the model treats them as such. The remaining 10 cells had no received P loading from either local or upstream contributions. Cells with no P loading from WRRF discharge that are nutrient impaired may be receiving P from non-point sources, such as fertilizer or biosolids application. Approximately half of the cells (66) had 84 % or greater of EP_R from local sources rather than upstream contributions. Only 27 cells had less than or equal to 12 % of their EP_R from local sources.

3.4. Case study: Wabash River in Indiana

A flow network is shown in Fig. 6 identifying all upstream sources of P loading to the grid cell that contains the outlet of the Wabash River case study region (cell 50607). All flows to cells that contain reaches of the river are mapped with a green star denoting there are no further upstream flows into that cell. Total EP_R was calculated based on each upstream P contribution from WRRF discharge. A total of 383 WRRFs in the 19 cells contain or contribute to different reaches of the Wabash River. The total EP_R at the mouth of the river was estimated at 4863 lb P-eq. Table 2 shows the lb of P-eq contributed to cell 50607 from each upstream emitting cell as a percent contribution to total EP_R.

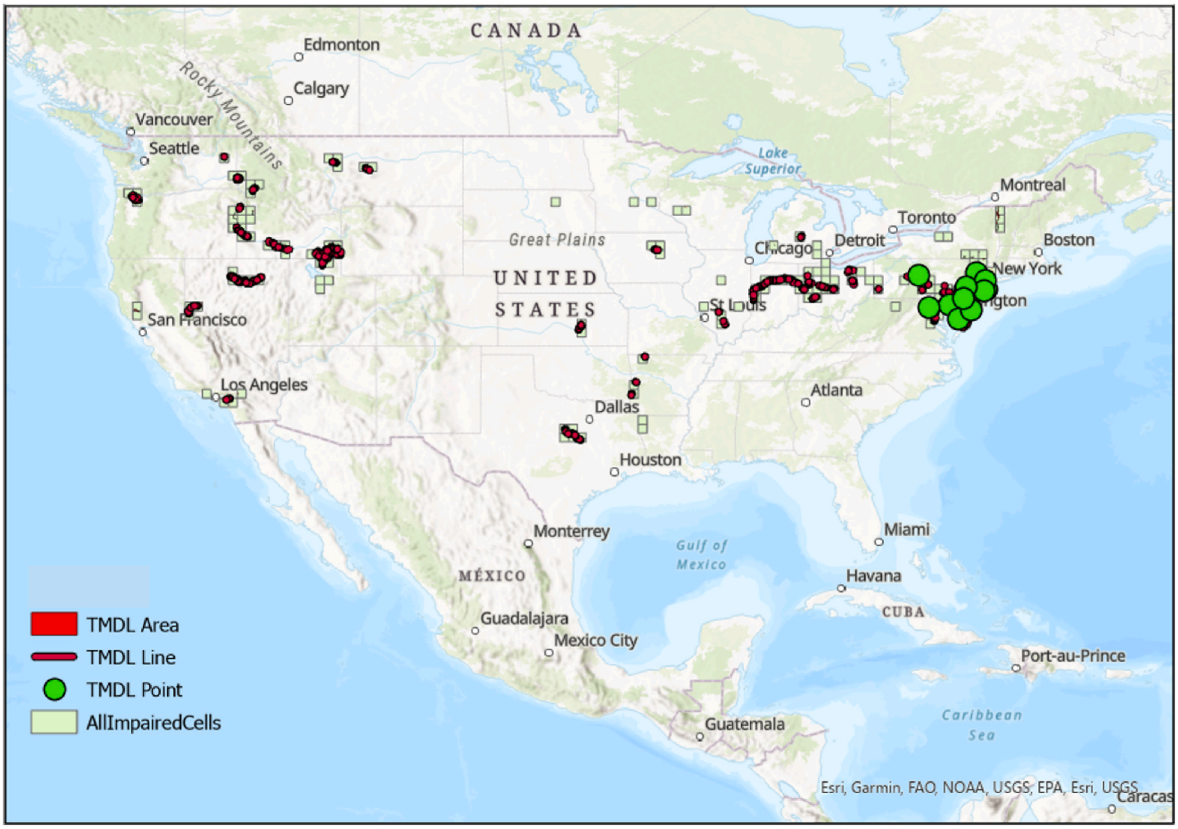

Fig. 4. 303(d) listed nutrient impaired waters in the U.S. intersected with grid cells.

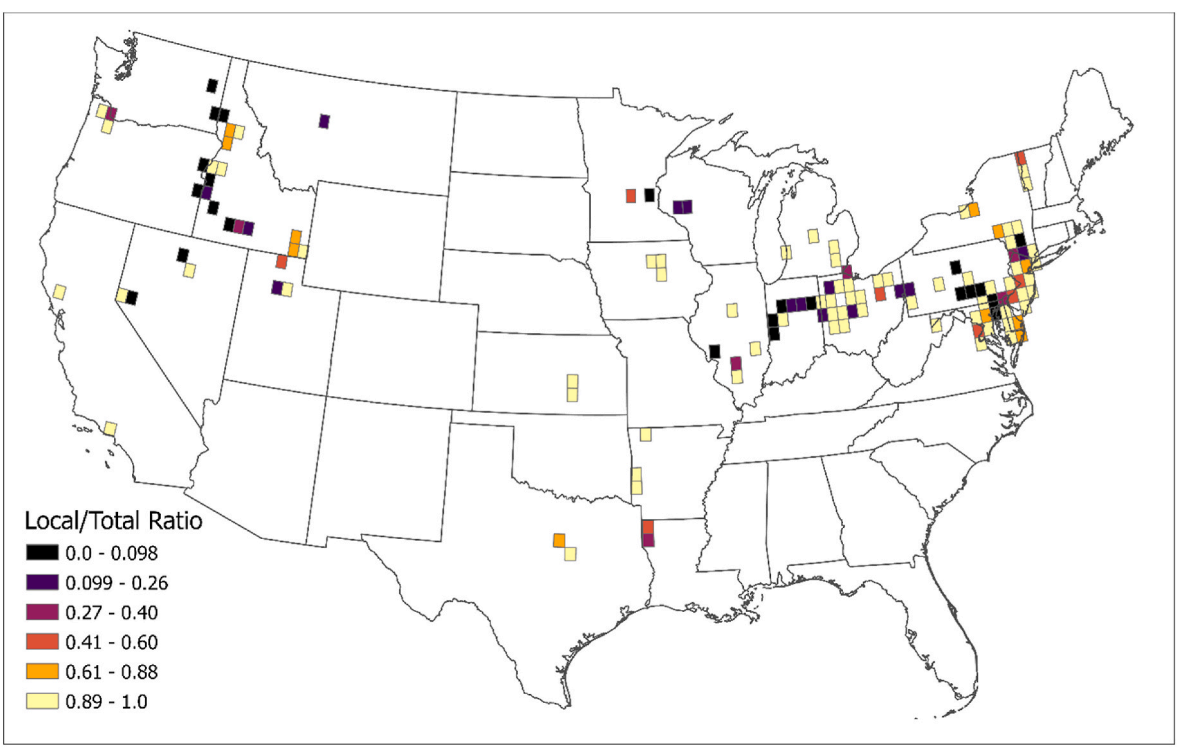

Fig. 5. Heat map of EP_R in 303(d) nutrient impaired waters.

Cells 50609, 50709, and 50714 contribute the most to spatially explicit EP in cell 50607. Cell 50609 contributes the largest percentage of EP_R (32 %) to the Wabash River. This cell contains most of the city of Indianapolis and contains 29 WRRFs (Table S2). Total P emissions in this cell from WRRF discharge is estimated at approximately 356,500 lb P annually. Of these P emissions, approximately 70 % comes from two

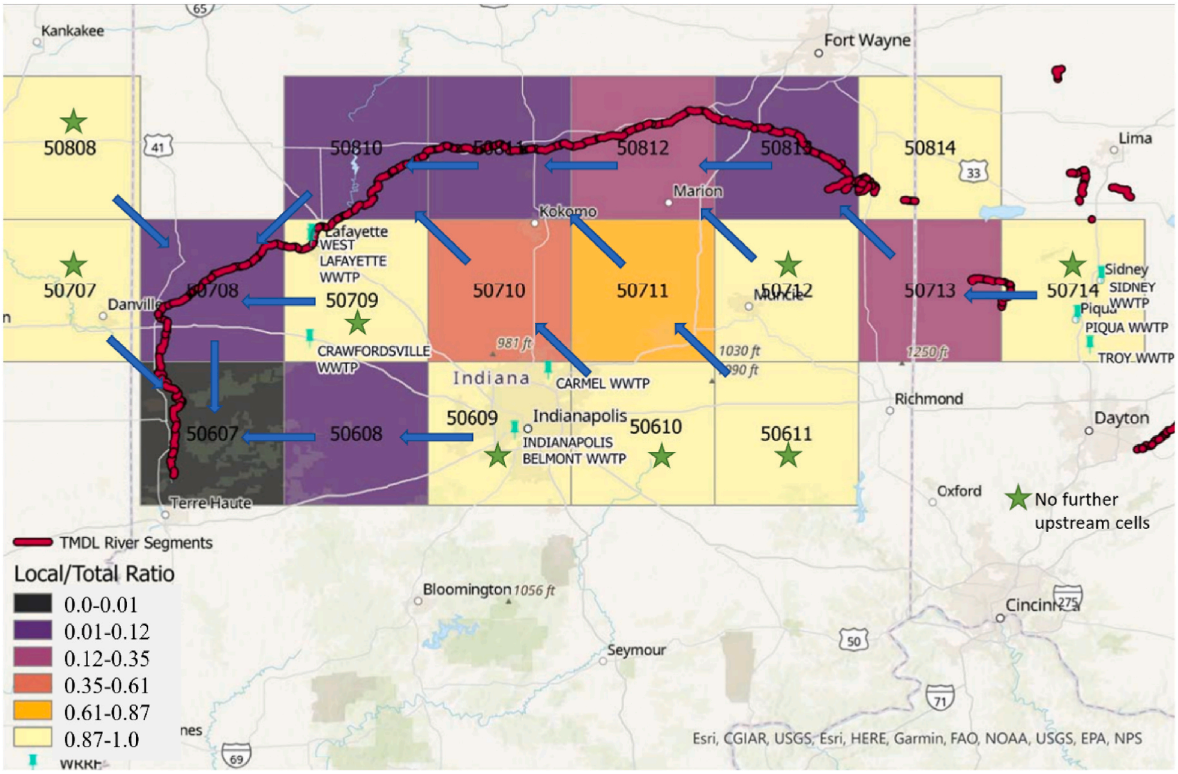

Fig. 6. Wabash River flow network with local to total EP contributions.

Table 2
Percent Contribution to EP_R to outlet of Wabash River case study region (cell 50607).

Emitting Cell ID	EP Loading to Receiving Cell 50607 (lb P-eq)	Percent Contribution to Total EP_R
50607	35.1	1 %
50608	112	2 %
50609	1540	32 %
50610	279	6 %
50611	217	4 %
50707	141	3 %
50708	36.1	1 %
50709	484	10 %
50710	164	3 %
50711	352	7 %
50712	187	4 %
50713	109	2 %
50714	492	10 %
50808	284	6 %
50810	87.0	2 %
50811	170	3 %
50812	118	2 %
50813	62.3	1 %

WRRFs: Indianapolis Belmont WRRF (56 %) and Carmel WRRF (14 %). Indianapolis Belmont WRRF has the highest design flow (125 million gallons per day, MGD). Carmel WRRF has a design flow of 14 MGD and all other treatment plants in this cell have a design flow of less than 10 MGD. Cells 50714 and 50709 are the second and third largest contributing cells to EP loading. Total annual phosphorus emissions in these cells from WRRF discharge is 142,955 and 92,062 lb, respectively. Cell 50714, which includes the city of Piqua, OH, has 22 WRRFs (Table S3). Nearly 90 % of P emissions in this cell come from 4 WRRFs: Sidney, Troy, Piqua and Minster WRRFs. The two largest contributors together make up almost 70 % of the P emissions from the cell.

All four treatment plants report an average P effluent concentration >1 mg/L, with Sidney reporting the highest P concentration at 5.2 mg/L. Sidney and Troy have the highest design flows (7 and 5 MGD, respectively) while the other WRRFs in this cell have design flows of less than 1 MGD. For Cell 50709, which includes Lafayette, IN, has 27 WRRFs (Table S4). Similar to cell 50714, approximately 90 % of P emissions are released from 4 WRRFs: Lafayette, Crawfordsville, West Lafayette, and Frankfort). The two plants with the highest P emissions contribute nearly 2/3 of the P emissions released from this cell. Unlike the WRRFs in the Piqua area, only one of the four WRRFs in the Lafayette region (Crawfordsville) has an average reported P effluent concentration of greater than 1 mg/L (3.1 mg/L average P effluent concentration). The highest contributing plant, Lafayette, has an average P effluent concentration of 0.74 mg/L but a design flow that is three times bigger than the next largest WRRF (West Lafayette).

This information can also be presented after modeling changes in P emissions from individual cells resulting from theoretical implementation of nutrient recovery and/or advanced treatment technologies in WRRFs to determine changes in P loadings to the Wabash River watershed. Fig. 7 shows the estimated potential changes that could be achieved in steady-state EP_R to the Wabash River watershed if P emissions from individual cells are uniformly reduced by 25 %.

Data points in this figure represent individual cells and are labeled based on the WRRF with the largest EP_R contribution they contain within their geographic boundary. For cells clustered near the origin, a 25 % change in their P emissions would change their annual P emissions by 20,000 lb P or less and result in changing overall watershed EP_R by less than 1000 lb P-eq. Thus, cells with a lower P emission reduction but higher change in watershed EP are the key cells to analyze. In other words, the greatest EP reduction can be achieved with a smaller change in P emissions within these key cells.

Changes in P emissions in the Indianapolis cell would have the greatest impacts to EP_R as this cell contributes nearly 1/3 of loading to the outlet of the Wabash River. However, based on our analysis, Piqua and Sidney achieve a EP_R reduction close to that of Indianapolis (3600 lb P-eq to 4200 lb equivalent, respectively) but with a less than half of the required reduction in lb of P emitted. A 25 % reduction in P emissions in

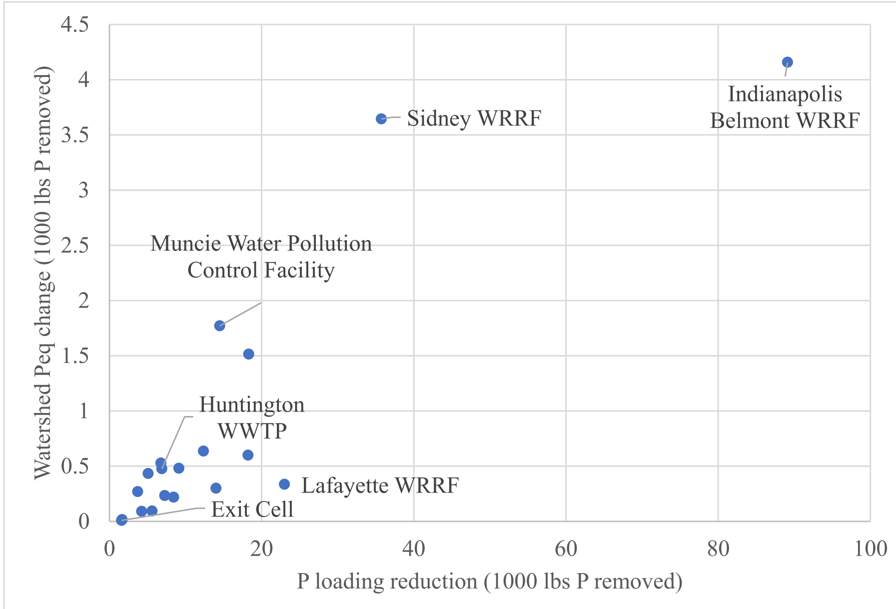

Fig. 7. EP_R reduction potential as a function of reduced P loading.

this cell could be achieved through advanced treatment/nutrient recovery processes implemented at one or more plants in this particular cell. For example, the Sidney WRRF has an average effluent P concentration of 5.2 mg P/L and an average flow of 4.5 MGD, resulting in approximately 70,500 lb P emitted per year. To achieve a 25 % reduction in these emissions, the P effluent concentration would need to be reduced to under 4 mg/L to reduce P emissions from this cell from approximately 70,500 lb P/year to 52,900 lb P/year. As the plant currently uses conventional activated sludge processes to treat wastewater, advanced treatment technologies, such as enhanced biological nutrient removal, could be used to lower the P concentration to below 4 mg/L (US EPA, 2007).

4. Conclusion

This study extends the evaluation of EP from the standard LCIA perspective of assigning the impact to the emitting cell only and provides a mechanism to extend the understanding of EP to an upstream contribution perspective. This analysis provides an estimation of key point-source P emissions and sources of EP to grid cells in the U.S. from P flows in WRRF discharge. An analysis of current spatially explicit EP_E estimates in the U.S. show EP_E comes from grid cells that have either high P emissions or high cumulative FFs. Some key regions include the Great Lakes area, areas in the Midwest, as well as some areas closer to arid regions such as Houston, TX and Utah. Changes in P flows to these cells achieved through nutrient recovery or advanced treatment technologies will be able to reduce P emissions in these cells. Thus, implementation of nutrient recovery or advanced treatment technologies in these locations would be most environmentally beneficial from an emissions perspective. With regards to received EP_R from WRRF discharge, most cells in the U.S. receive their P loading from local emissions, showing that local intervention may have the most significant impact to mitigating EP_R in these cells. However, there are cells in which local loadings are not the highest contributing factor to EP_R loadings, but rather P emissions from upstream cells. The case study shows how this data can be further disaggregated to identify key cells contributing to a receiving cell and thus identifying WRRFs that may be contributing most to P emissions and EP_R from WRRF discharge. This study shows how this approach can be used to analyze a receiving cell, such as one containing 303(d) nutrient impaired water, and determine upstream sources of P that can be further linked to specific WRRFs.

CRediT authorship contribution statement

Karla G. Morrissey: Writing – original draft, Visualization, Methodology, Investigation, Formal analysis, Data curation, Conceptualization. **Andrew D. Henderson:** Writing – review & editing, Validation, Supervision, Investigation, Formal analysis, Data curation. **John Zimmerman:** Methodology, Data curation. **Greg Thoma:** Writing – review & editing, Supervision, Software, Resources, Project administration, Funding acquisition.

5. Limitations

As shown in several figures, the approach used in this manuscript to identify sources of eutrophying emissions is based on a fate model suitable for large-scale assessments. Here, we apply it at the national level and demonstrate the analysis through a case study. The limitations of the underlying fate model are applicable here, including that model does not include a soil fate component; therefore, the irrigation effects are not captured. Furthermore, the model is limited to regions of the U.S. where there is a significant flow of water through the system. The approach is not yet well-suited to characterizing EP in much of the arid and semiarid western U.S. In such areas, it is likely that particulate-bound phosphorus will be slowly moved downstream by ephemeral flows. As large flows are necessary to mobilize particles, it's difficult to assess the degree to which the model is underestimating P flows. The model operates with an annual timestamp, so sub year, seasonal, variability is not captured. The principles used in this work will be applicable if the data and models are available at higher spatiotemporal resolution. Higher resolution modeling would, for example, allow the evaluation of recovery options and tradeoffs among nearby (< about 50 km, in the current model) WRRFs. Lastly, the work does not include non-point source P flows, which limits our ability to paint a full picture of EP in the U.S. Within WWT, some nutrient recovery technologies have shown that P reductions are primarily realized in sludge rather than liquid effluent. Therefore, it is important to include P flows of land application of sludge to capture the full environmental benefits that can be achieved from nutrient recovery technology. Future studies should build on this work to include these P flows when this data is made available.

Declaration of competing interest

The authors declare that they have no known competing financial interests or personal relationships that could have appeared to influence the work reported in this paper.

Acknowledgements

We are grateful for research funding provided by U.S. NSF Award #1739473 for the project titled, "INFEWS/T3: Critical Nutrient Recovery and Reuse: Nitrogen and Phosphorus Recycling from Wastewaters as Struvite Fertilizer."

Appendix A. Supplementary data

Supplementary data to this article can be found online at https://doi.org/10.1016/j.jclepro.2025.145536.

Data availability

Data will be made available on request.

References

al Rawashdeh, R., Maxwell, P., 2011. The evolution and prospects of the phosphate industry. Miner. Econ 24, 15–27. https://doi.org/10.1007/s13563-011-0003-8.

Amann, A., Zoboli, O., Krampe, J., Rechberger, H., Zessner, M., Egle, L., 2018. Environmental impacts of phosphorus recovery from municipal wastewater. Resour. Conserv. Recycl. 130, 127–139. https://doi.org/10.1016/j.resconrec.2017.11.002.

Bhat, S.U., Qayoom, U., 2021. Implications of sewage discharge on freshwater ecosystems. In: Sewage - Recent Advances, New Perspectives and Applications. IntechOpen. https://doi.org/10.5772/intechopen.100770.

Bulle, C., Margni, M., Patouillard, L., Boulay, A.-M., Bourgault, G., De Bruille, V., Cao, V., Hauschild, M., Henderson, A., Humbert, S., Kashef-Haghighi, S., Kounina, A., Laurent, A., Levasseur, A., Liard, G., Rosenbaum, R.K., Roy, P.-O., Shaked, S., Fantke, P., Jolliet, O., 2019. IMPACT world+: a globally regionalized life cycle impact assessment method. Int. J. Life Cycle Assess. 24, 1653–1674. https://doi.org/10.1007/s11367-019-01583-0.

Chorus, I., Spijkerman, E., 2021. What colin reynolds could tell Us about nutrient limitation, N:P ratios and eutrophication control. Hydrobiologia 848, 95–111. https://doi.org/10.1007/s10750-020-04377-w.

Chowdhury, R.B., Moore, G.A., Weatherley, A.J., Arora, M., 2014. A review of recent substance flow analyses of phosphorus to identify priority management areas at different geographical scales. Resour. Conserv. Recycl. 83, 213–228. https://doi.org/10.1016/j.resconrec.2013.10.014.

Cordell, D., Drangert, J.-O., White, S., 2009. The story of phosphorus: global food security and food for thought. Glob. Environ. Chng., Traditional Peoples and Climate Change 19, 292–305. https://doi.org/10.1016/j.gloenvcha.2008.10.009.

Corominas, Ll, Foley, J., Guest, J.S., Hospido, A., Larsen, H.F., Morera, S., Shaw, A., 2013. Life cycle assessment applied to wastewater treatment: state of the art. Water Res. 47, 5480–5492. https://doi.org/10.1016/j.watres.2013.06.049.

de Andrade, M.C., Ugaya, C.M.L., de Almeida Neto, J.A., Rodrigues, L.B., 2021. Regionalized phosphorus fate factors for freshwater eutrophication in Bahia, Brazil: an analysis of spatial and temporal variability. Int. J. Life Cycle Assess. 26, 879–898. https://doi.org/10.1007/s11367-021-01912-2.

Dodds, W.K., Smith, V.H., 2016. Nitrogen, phosphorus, and eutrophication in streams. Inland Waters 6, 155–164. https://doi.org/10.5268/IW-6.2.909.

Dodds, W.K., Bouska, W.W., Eitzmann, J.L., Pilger, T.J., Pitts, K.L., Riley, A.J., Schloesser, J.T., Thornbrugh, D.J., 2009. Eutrophication of U.S. freshwaters: analysis of potential economic damages. Environ. Sci. Technol. 43, 12–19. https://doi.org/10.1021/es801217q.

Dong, Y., Cheng, X., Li, C., Xu, L., 2023. Spatially eutrophication potential and policy implication of nitrogen emission for surface water: a case study in guangzhou city, China. J. Environ. Manag. 342, 118336. https://doi.org/10.1016/j.jenvman.2023.118336.

Egle, L., Rechberger, H., Krampe, J., Zessner, M., 2016. Phosphorus recovery from municipal wastewater: an integrated comparative technological, environmental and economic assessment of P recovery technologies. Sci. Total Environ. 571, 522–542. https://doi.org/10.1016/j.scitotenv.2016.07.019.

Florczyk, A.J., Ehrlich, D., Freire, S., Kemper, T., Maffenini, L., Melchiorri, M., Melchiorri, M., Pesaresi, M., Politis, P., Schiavina, M., Sabo, F., Zanchetta, L., 2019. GHSL Data Package 2019, EUR 29788 EN. Publications Office of the European Union, Luxembourg. ISBN 978-92-76-13186-1.

JRC, Freire, S., Corbane, C., Zanchetta, L., Schiavina, M., Politis, P., Kemper, T., Ehrlich, D., Pesaresi, M., Maffenini, L., Florczyk, A.J., Melchiorri, M., Sabo, F., 2019. GHSL Data Package 2019: Public Release GHS P2019. Joint Research Center, Luxembourg. https://data.europa.eu/doi/10.2760/290498.

Helmes, R.J.K., Huijbregts, M.A.J., Henderson, A.D., Jolliet, O., 2012. Spatially explicit fate factors of phosphorous emissions to freshwater at the global scale. Int. J. Life Cycle Assess. 17, 646–654. https://doi.org/10.1007/s11367-012-0382-2.

Henderson, A.D., 2015. Eutrophication. In: Hauschild, M.Z., Huijbregts, M.A.J. (Eds.), Life Cycle Impact Assessment. Springer, Netherlands, Dordrecht, pp. 177–196. https://doi.org/10.1007/978-94-017-9744-3_10.

Henderson, A.D., Niblick, B., Golden, H.E., Bare, J.C., 2021. Modeling spatially resolved characterization factors for eutrophication potential in life cycle assessment. Int. J. Life Cycle Assess. 26, 1832–1846. https://doi.org/10.1007/s11367-021-01956-4.

Jarvie, H.P., Sharpley, A.N., Flaten, D., Kleinman, P.J.A., Jenkins, A., Simmons, T., 2015. The pivotal role of phosphorus in a resilient water-energy-food security nexus. J. Environ. Qual. 44, 1049–1062. https://doi.org/10.2134/jeq2015.01.0030.

Johansson, K., Perzon, M., Fröling, M., Mossakowska, A., Svanström, M., 2008. Sewage sludge handling with phosphorus utilization – life cycle assessment of four alternatives. J. Clean. Prod. 16, 135–151. https://doi.org/10.1016/j.jclepro.2006.12.004.

Jolliet, O., Müller-Wenk, R., Bare, J., Brent, A., Goedkoop, M., Heijungs, R., Itsubo, N., Peña, C., Pennington, D., Potting, J., Rebitzer, G., Stewart, M., de Haes, H.U., Weidema, B., 2004. The LCIA midpoint-damage framework of the UNEP/SETAC life cycle initiative. Int J LCA 9, 394–404. https://doi.org/10.1007/BF02979083.

Jönsson, H., Stintzing, A.R., Vinnerås, B., Salomon, E., 2004. Guidelines on the Use of Urine and Faeces in Crop Production. EcoSanRes Publications. Stockholm Environment Institute, Stockholm, Sweden.

Lam, K.L., Zlatanović, L., van der Hoek, J.P., 2020. Life cycle assessment of nutrient recycling from wastewater: a critical review. Wat. Res. 173, 115519. https://doi.org/10.1016/j.watres.2020.115519.

Linderholm, K., Tillman, A.-M., Mattsson, J.E., 2012. Life cycle assessment of phosphorus alternatives for Swedish agriculture. Resour. Conserv. Recycl. 66, 27–39. https://doi.org/10.1016/j.resconrec.2012.04.006.

Moore, R.B., Johnston, C.M., Smith, R.A., Milstead, B., 2011. Source and delivery of nutrients to receiving waters in the northeastern and mid-atlantic regions of the United States. J. Am. Water Resour. Assoc. 47, 965–990. https://doi.org/10.1111/j.1752-1688.2011.00582.x.

Morrissey, K.G., English, L., Thoma, G., Popp, J., 2022. Prospective life cycle assessment and cost analysis of novel electrochemical struvite recovery in a U.S. wastewater treatment plant. Sustainability 14, 13657. https://doi.org/10.3390/su142013657.

Preisner, M., Neverova-Dziopak, E., Kowalewski, Z., 2021. Mitigation of eutrophication caused by wastewater discharge: a simulation-based approach. Ambio 50, 413–424. https://doi.org/10.1007/s13280-020-01346-4.

Preston, S.D., Alexander, R.B., Schwarz, G.E., Crawford, C.G., 2011a. Factors affecting stream nutrient loads: a synthesis of regional SPARROW model results for the Continental United States. J. Am. Water Resour. Assoc. 47, 891–915. https://doi.org/10.1111/j.1752-1688.2011.00577.x.

Preston, S.D., Alexander, R.B., Wolock, D.M., 2011b. Sparrow modeling to understand water-quality conditions in major regions of the United States: a featured collection Introduction 1. J. Am. Water Resour. Assoc. 47, 887–890. https://doi.org/10.1111/j.1752-1688.2011.00585.x.

Rahman, S., Chowdhury, R.B., D'Costa, N.G., Milne, N., Bhuiyan, M., Sujauddin, M., 2019. Determining the potential role of the waste sector in decoupling of phosphorus: a comprehensive review of national scale substance flow analyses. Resour. Conserv. Recycl. 144, 144–157. https://doi.org/10.1016/j.resconrec.2019.01.022.

Remy, C., Jossa, P., 2015. Sustainable sewage sludge management fostering phosphorus recovery and energy efficiency: life cycle assessment of selected processes for P recovery from sewage sludge, sludge liquor, or ash (no. D 9.2), WP09: Comparative life cycle assessment of treatment-recovery paths. KWB; European Commission within the Seventh Framework Programme Grant agreement No., 308645. Berlin, Germany.

Robertson, D.M., Saad, D.A., 2019. Spatially Referenced Models of Streamflow and Nitrogen, Phosphorus, and suspended-sediment Loads in Streams of the Midwestern United States (USGS Numbered Series No. 2019–5114), Spatially Referenced Models of Streamflow and Nitrogen, Phosphorus, and suspended-sediment Loads in Streams of the Midwestern United States, Scientific Investigations Report. U.S. Geological Survey, Reston, VA. https://doi.org/10.3133/sir20195114.

Rodriguez-Garcia, G., Frison, N., Vázquez-Padín, J.R., Hospido, A., Garrido, J.M., Fatone, F., Bolzonella, D., Moreira, M.T., Feijoo, G., 2014. Life cycle assessment of nutrient removal technologies for the treatment of anaerobic digestion supernatant and its integration in a wastewater treatment plant. Sci. Total Environ. 490, 871–879. https://doi.org/10.1016/j.scitotenv.2014.05.077.

Sena, M., Hicks, A., 2018. Life cycle assessment review of struvite precipitation in wastewater treatment. Resour. Conserv. Recycl. 139, 194–204. https://doi.org/10.1016/j.resconrec.2018.08.009.

Sena, M., Seib, M., Noguera, D.R., Hicks, A., 2021. Environmental impacts of phosphorus recovery through struvite precipitation in wastewater treatment. J. Clean. Prod. 280, 124222. https://doi.org/10.1016/j.jclepro.2020.124222.

US EPA, 2007. Advanced Wastewater Treatment to Achieve Low Concentration of Phosphorus (No. EPA 910-R-07-002). United States Environmental Protection Agency, Office of Water and Watersheds, Seattle, WA.

US EPA, 2015a. A Compilation of Cost Data Associated with Impacts and Control with Nutrient Pollution (No. EPA 820-F-15-096). United States Environmental Protection Agency, Office of Water, Washington, DC, USA.

US EPA, 2015b. 303(d) Listed Impaired Waters [WWW Document]. United States Environmental Protection Agency, Office of Research and Development. https://www.epa.gov/ceam/303d-listed-impaired-waters. accessed 11.20.22.

US EPA, 2020. National Rivers and Streams Assessment 2013–2014: a Collaborative Survey (No. EPA 841-R-19-001), National Aquatic Resource Surveys. United States Environmental Protection Agency, Office of Water and Office of Research and Development, Washington, DC, USA.
US EPA, 2022a. National Lakes Assessment: the Third Collaborative Survey of Lakes in the United States (No. EPA 841-R-22-002), National Aquatic Resource Surveys. United States Environmental Protection Agency, Office of Water and Office of Research and Development, Washington, DC, USA.
US EPA, 2022b. Nutrient modeling (hypoxia task force search). https://echo.epa.gov/trends/loading-tool/hypoxia-task-force-nutrient-model accessed 11.20.22.
Wang, X., Daigger, G., de Vries, W., Kroeze, C., Yang, M., Ren, N.-Q., Liu, J., Butler, D., 2019. Impact hotspots of reduced nutrient discharge shift across the globe with population and dietary changes. Nat. Commun. 10, 2627. https://doi.org/10.1038/s41467-019-10445-0.
Wurtsbaugh, W.A., Paerl, H.W., Dodds, W.K., 2019. Nutrients, eutrophication and harmful algal blooms along the freshwater to marine continuum. WIREs Water 6, e1373. https://doi.org/10.1002/wat2.1373.
Zhuang, Y., Liu, X., Zhou, J., Sheng, H., Yuan, Z., 2024. Multidirectional fate path model to connect phosphorus emissions with freshwater eutrophication potential. Environ. Sci. Technol. 58, 11675–11684. https://doi.org/10.1021/acs.est.4c01205.
Zimmerman, J., 2021. Identification of Phosphorous Loading Point Source Facilities to 303(d) Listed Nutrient Impaired Waters Through Watershed Delineation Using Arcgis for Life Cycle Assessment Applications (Undergraduate Thesis). University of Arkansas, Fayetteville, Arkansas.